# Brain Cancer classification Based on Features and Artificial Neural Network

**Nidahl K. El Abbadi[1], Neamah E. Kadhim[2]**

Computer Science Department, Education College, University of Kufa, Najaf, Iraq[1]

Computer Science Department, Science College, University of Babylon, Babylon, Iraq[2]

**Abstract**: MRI (Magnetic resonance Imaging) brain tumor images Classification is a difficult task due to the variance and complexity of tumors. This paper proposed techniques to classify the MR human brain images. The proposed classification technique consists of three stages, namely, pre-processing, feature extraction and selection, and classification. Features are extracted by using the gray level co-occurrence matrices and the gray level run length matrices (GLCM & GLRLM), 18 features were determined from the image, then selected the most important features that saved to the database. In the final stage, the classifier based on probabilistic neural network (PNN) have been used to classify MRI brain images, the proposed algorithm is trained with 50 images of (Sarcoma, Anaplastic Astrocytoma, Meningioma, and Benign) and tested with 65 images. The accuracy of this method was up to 98%.

**Keywords:** MRI, brain tumor, classification, image processing, PNN.

## I. INTRODUCTION

In recent years, abrain tumor is classified as one of the main diseases for growing death rate amongst kids and adults. The MRI is widely used by most of the physicians to identify the brain tumor in the present days. It's found that the whole number of individuals that hardship and death because of brain tumors has been improved to 300 for each year through previous few periods [1].

Identification of the tumor regions accurately from the MRI is considered to be a challenging job for the physicians. The image processing tools are used to accurately classify the tumor. Many researchers reported various techniques for identification of tumor region [2].

The tumor is due to the uncontrolled growth of the tissues in any part of the body. The brain tumors are classified as benign (Non-cancerous) which means they do not spread or invade the surrounding tissue and malignant (cancerous) which spreads or invades the surrounding tissue. It is categorized as aprimary and secondary tumor. Different types of thealgorithms were developed for brain tumor detection. [3]

Helping radiologists in reading medical images is the key notion from computer assisted diagnosis system by way of using devoted computer systems to offer "second opinions". Computer aided (CAD) system as show in researches on CAD schemes and medical technology can help to develop detection precision from the radiologists, lighten the load of accumulative work, and reduce the loss of the discovery of cancer rates because of exhaustion, ignored or data overloaded. The ending medical decision is prepared by the radiologists. As a result, radiologists suppose these systems be able to develop the diagnostic capabilities based upon interactive effects amongst the computer and the radiologist and with machine learning methods and medicinal image analysis [4].

There are over 100 classes of main brain tumors, a number of them very infrequent. On the other hand, not all brain tumors, or even all malignant brain tumors, are always deadly. With surgical treatment, radiation treatment, and chemotherapy, many types of tumors respond very well to the therapy and may even be treated. While many of the more common tumors, such as gliomas, are not typically cured by surgical resection, there are time-consuming term survivors now than ever before, as a new therapy have been presented [5].

## II. RELATED WORKS

A.Lakshmi and Dr.T.Arivoli [6] proposed a computer assisted method to improve the diagnosis / detection of abrain tumor. The suggested work involves four phases that are: pre-processing, extract the features, then artificial neural with fuzzy inference system ANFIS Classifier is used, then the morphological processes for discovering, segmenting and detecting the brain tumor areas. First the preprocessing is carried out before going to segmentation since pre-processing prepares the image to be prepared for segmentation.

Nalbalwar et al. [7] have produced a recognition and classification methods for brain cancer. These proposed methods use techniques based on the computer to discover blocks of the tumor and then classify the category of the tumor using ANN in MRI of a various number of patients that suffer from astrocytoma tumor type in the brain. ANN has been used as a classifier to the brain MR images classification that produces good classification accuracy as compared to other classifiers.

John [8] has presented an effective method of brain tumor classification, where, the actual MRI images which classified to the benign or malignant (non-cancerous or

cancerous) brain tumor. The offered technique compromise of three stages. The DWT that first working in order to dissolve the MR image to the various levels of coefficients, then the GLCM gray matrices is calculated, then the features that based on texture like energy, homogeneity, correlation, contrast and entropy which are calculated from this matrices. The calculated features then applied to an ANN that based on probabilistic PNN for additional classification and detection of thetumor.

## III. METHODOLOGY OF THE PROPOSED METHOD

The proposed approach is shown in figure 1 below. There are three main steps in the proposed method:
(1) Preprocessing (2) Feature extraction and selection (3) classification.

### 1. MR brain tumor database acquisition
The brain images MRI (brain tumor MRI and normal MRI) have been obtained from different medical centers (Hilla Center for MRI, MR Imaging of Neoplastic Central Nervous System and whole brain tumor Atlas) in JPEG format.
The MRI images that have been obtained from these centers are:
A. Sarcoma (25 image).
B. Anaplastic Astrocytoma (36 image).
C. Meningioma (30 image).
D. Metastatic bronchogenic carcinoma (20 image)
E. Benign (15 image)

The MR images that weretaken from these centers in JPEG, TIF and BMP files format. These images first resizing to be in the same size and in a specific format to be generalized in all computations and comparatives, then are stored in a data base.

### 2. MRI De-noising and Enhancement
The objectives of these algorithms are to perform noise reduction, or de-noising, based on morphology operation techniques. The MRI Brain image first loaded from the database, then the noise is removed from the MRI image with preserved the edge details and produce the image with good enhancement.
The proposed algorithm depends on implementing of mathematical morphology operations eroding and dilation. These operations process the image according to shape by hit or miss transformation and depending on the selected structure element. The algorithm processes the noises image after dividing the image into three channels (Red, Green, and Blue), and in the end concatenation these three sub images to produce a final de-noising image.

### 3. Features extraction and selection
Features extraction encompasses simplifying the amount of features necessary to refer to a large group of data accurately and preserves its content. In this proposed work the features extraction depends on the following features:

### A. First order statistical features
Related to frequency of appearance of each gray level (histogram)in the region of interest (ROI) [11,12]:

a) Mean value.

$$m = \frac{\sum_i \sum_j g(i,j)}{N}$$

b) Standard deviation:

$$std = \sqrt{\frac{\sum_i \sum_j (g(i,j) - m)^2}{N}}$$

c) Skewness

$$sk = \frac{1}{N} \frac{\sum_i \sum_j (g(i,j) - m)^3}{std^3}$$

d) Kurtosis:

$$k = \frac{1}{N} \frac{\sum_i \sum_j (g(i,j) - m)^4}{std^4}$$

### B. Computing Gray level Run length matrix (GLRLM)
It is necessary to interpret tissue appearance when examining the images in medicinal, based on different properties such as regularity, smoothness, homogeneity, and grain. These characteristics are associated with the localized intensity differences and be able to take through using different texture measurements. Statistics of run-length take the roughness at the texture in identified ways (guidelines/directions). Then can define the run by way of a series in succeeding pixels that take the similar intensities (levels of gray) over a particular linear direction.
The textures that have additional small runs with similar levels of gray is a good texture, but the textures that have to be more long runs through thevarious gray level is a roughness.
We compute GLRLM in four directions (0°, 45°, 90°, and 135°) to produce four matrixes, and on MRI image that quantized to four bits (16 gray level).

As soon as the matrices of run-length are computed via each direction, a number of texture features are computed to release the texture properties and distinguish among various textures. These features are computed depending on each direction. From these matrices (run-length), seven features are extracted, briefly description of each of them as below[13,14]:

i. Short run emphasis (SRE):Gauge the scattering of small runs.

$$SRE = \frac{\sum_{i=1}^{N_g} \sum_{j=1}^{N_r} \frac{r(i,j)}{j^2}}{\sum_{i=1}^{N_g} \sum_{j=1}^{N_r} r(i,j)}$$

ii. Long run emphasis (LRE): Head for confirming (emphasize) runs that are long and it is large for smoother ROI.

$$LRE = \frac{\sum_{i=1}^{N_g} \sum_{j=1}^{N_r} j^2 r(i,j)}{\sum_{i=1}^{N_g} \sum_{j=1}^{N_r} r(i,j)}$$

iii. Gray level non-uniformity (GLNU): The ROI that having several times of runs of the similar value of gray level.

$$GLNU = \frac{\sum_{i=1}^{N_g} \left( \sum_{j=1}^{N_r} r(i,j) \right)^2}{\sum_{i=1}^{N_g} \sum_{j=1}^{N_r} r(i,j)}$$

iv. Run Percentage (RP): The gauge of the homogeneity/similarity and dispersion of runs into the image in a particular way.

$$RP = \frac{\sum_{i=1}^{N_g} \sum_{j=1}^{N_r} r(i,j)}{P}$$

**C. Calculate the co-occurrence matrix of gray-level (GLCM):**

Co-occurrence matrix of gray level features supposes that the information of the texture into the image exists at the spatial relationships among the pixels in the image. First GLCM has computed the features then statistically obtained from it.

GLCM is created by computing how many times a pixel that has x gray-level intensity that happens horizontally neighboring to the pixel that has y value. Each component (x,y) into the GLCM identifies the total no. that the pixel which has x value happened in a horizontal neighboring to a pixel which has y value through direction. For calculating the GLCM need to set some parameters such as[15]:

**'GrayLimits'**: [small large], that states how the gray levels values in "I" are scaled.

**'NumLevels'**: the no. of the gray-levels that using when the values of the grayscale in the image are scaling, then identified by this integer value.

**'Offset'**: anarray of integers identifying the distance between the pixels of interest and its surrounding pixels or neighbor. For the reason that the offset is frequently stated by way of the angle (figure 1): Offset = [0 1; -1 1; -1 0; -1 -1]

**'Symmetric':** Boolean value that describes the ordering of values in the pixel pairs that must be considered. For example, when this value setting to 'true', gray co-occurrence matrices counts both 1, 2 and 2, 1 pairings when calculating the no. of times the value 1 is adjacent to the value 2.
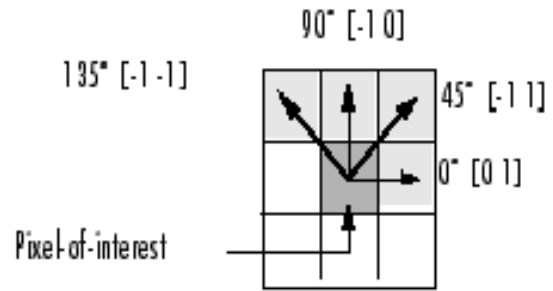


Figure 1. Representation of offset parameter

The texture features that are extracted from each of the four normalized matrices gray-level co-occurrence matrices (GLCM) so that the sum of its elements is equivalent to 1. Each component (r,c) in the normalized GLCM is the joined probability occurrence of pixel pairs with a defined spatial correlation having values r and c of gray level in the image. Then stored in the database. The features that extracted from GLCM as the following [16,17]:

1. Angular Second Moment (Energy): Energy gauges the no. of reiterated pairs, or indicates how a gray level elements are distributed.

$$ASM = \sum_{i=0}^{N_g-1} \sum_{j=0}^{N_g-1} \left( p(i,j) \right)^2$$

2. Contrast:
The contrast feature measures the local contrast or variations presented in an image:

$$CON = \sum_{n=0}^{N_g-1} n^2 \left\{ \sum_{i=0}^{N_g-1} \sum_{j=0}^{N_g-1} \left( p(i,j) \right)^2 \right\}, |i-j| = n$$

3. Inverse Difference Moment IDM or (Homogeneity):Homogeneity is a straight measurement of the local similarity of a gray level in an image:

$$IDM = \sum_{i=0}^{N_g-1} \sum_{j=0}^{N_g-1} \frac{p(i,j)}{1+(i-j)^2}$$

4. Entropy:A gray-level distribution randomness is computed in this measures:

$$ENT = \sum_{i=0}^{N_g-1} \sum_{j=0}^{N_g-1} p(i,j) \log \left( p(i,j) \right)$$

5. Correlation COR:Correlation is a standard measure of image contrast to evaluate linear dependent on the gray levels of adjacent pixels:

$$COR = \frac{\sum_{i=0}^{N_g-1} \sum_{j=0}^{N_g-1} (ij)p(i,j) - m_x m_y}{\sigma_x \sigma_y}$$

6. Sum of squares (SSQ)

$$SSQ = \sum_{i=0}^{N_g-1} \sum_{j=0}^{N_g-1} (1-m)^2 p(i,j)$$

7. Sum average (SAVE)

$$SAVE = \sum_{i=2}^{2N_g} i p_{x+y}(i)$$

Where $p_{x+y}$ represent:

$$p_{x+y}(k) = \sum_{i=1}^{N_g} \sum_{j=1}^{N_g} p(i,j), i+j = k, k = 2,3,\dots,2N_g$$

8. Sum entropy (SENT)

$$SENT = -\sum_{i=2}^{2N_g} p_{x+y}(i) \log\left(p_{x+y}(i)\right)$$

9. Sum variance (SVAR) and Difference variance (DVAR)

$$SVAR = -\sum_{i=2}^{2N_g} (i - SENT)^2 p_{x+y}(i)$$

$$SVAR = -\sum_{i=2}^{2N_g} (i - SENT)^2 p_{x+y}(i)$$

10. Difference entropy (DENT)

$$DVAR = \sum_{i=2}^{2N_g} (i - SAVE)^2 p_{x-y}(i)$$

Where $p_{x-y}$ is

$$p_{x-y}(k) = \sum_{i=1}^{N_g} \sum_{j=1}^{N_g} p(i,j), |i-j| = k, k = 2,3,\dots,N_g - 1$$

## D. Features selection

In this stage, the features are calculated for many classes type of abnormal MRI brain images and saved them in a data base, also saved the result of these features calculated for normal MRI brain images.

To see differences and similarity between these values, the features values have been retrieved from a database that corresponds to each class type and they have been used to differentiate between different types of classes of abnormal MRI brain images.

From analyzing the computed feature of all classes type and with experiments, the most importance feature that can produce accurate classification are: Skewness, Kurtosis, Short run emphasis (SRE), Gray level non-uniformity (GLNU), Run length non uniformity (GLNU), Run percentage (RP), Contrast CON, Inverse Difference Moment IDM(Homogeneity), Correlation COR, Sum of squares (SSQ), Sum average (SAVE), Sum entropy (SENT),Sum variance (SVAR) and Difference variance (DVAR) and Difference entropy (DENT). These features produce good values, that can accurately for classifying the brain tumor MRI images, therefore we are selected them in classification modal. The other features: Mean zvalue, Standard deviation, Entropy, Long run emphasis (LRE) and Angular Second Moment ASM (Energy) are rejected because of that values they produce overlapping between classes types samples of brain tumor MRI images and they don't can use to isolate these classes.

## E. PNN Classification Phase

Artificial Neural Networks (ANNs) have been developed for a wide range of applications such as function approximation, feature extraction, optimization, and classification. In particular, they have been developed for image enhancement, segmentation, registration, feature extraction, and object recognition and classification. Among these, object recognition and image classification are more important as it is a critical step for high-level processing such as brain tumor classification. Multi-Layer Perceptron (MLP)[18].

The artificial networks for pattern recognition are fed forward networks that be able to be trained to be able for classifying net inputs according to the target classes. The information of a target for these networks should involve of vectors which all have zeros 0s values excepting for a 1 in position i, where this position is to the class they are to represent.

## i. Architecture:

The proposed network architecture consists of the following four layers:
a) Input layer: consist of thirteen nodes represents the inputs vector that enters to the network, here it's a features vector that selected to classify the classes of brain tumor MRI.
b) The first layer in the hidden: pattern layer, involve of twenty states.
c) The second layer in the hidden: summation layer, involve of five states.

d) Output layer: involve of five states that represent no. of classes (brain tumor type) that need the network to classify them. The output of the network are five values, each value represents theprobability of each input vectors belonging to any one of five classes. The output vector of the network consist of five probabilities (between 0 and 1), and the net take the class belongs to higher (maximum) probability.

## ii. Training set:
The network uses supervised learning method, then it need training set to be as (input, target) vectors. When the input features vector sample and target as vectors of five values one setting to one value and the others setting to zeros, for example, the target vector [1 0 0 0 0] refer to that feature is belonging to class one.

## iii. Activation (Transfer) function:
The network uses 'Hyperbolic tangent sigmoid transfer function' (tan sigmoid function) as a function for the transfer of the net. The output of the layers is computed through these Transfer functions and from its net input( hidden layer one and two). This function mathematically represented as:

$$tanget(s) = 2/(1 + e(-2*s)) - 1$$

## iv. Training function:
The network uses Training function **'trainlm'** Levenberg-Marquardt back propagation, trainlm is a function for teaching the network through updating the bias and weights values according to optimization method of LevenbergMarquardt.
If the transfer functions of the net have derivative functions, then this function is appropriate to learn the network.
The "trainlm" learning function need to set some of theimportant parameters that are:
− Max no. of times that the net be trained (1000)
− The performance of the train (0).
− Max no. of validate failures (6).
− The gradient of Mini Performance (1e-7).
− Initializing the value of mu to (0.001).
− Decreasing of mu factor (0.1).
− Incremented of mu factor by (10).
− Max value of mu is (le10).

The Jacobian jX of performance "perf" is computed depending on the bias and weight variables X. Each variable is adjusted according to the "Levenberg-Marquardt",
jj = jX * jX
je = jX * E
dX = -(jj+I*mu) \ je

Where E represent all errors and I is the identity matrices. The mu adaptive value is increased via mu_inc value till the adjustment above produces the performance value to be reduced. Then the alteration is then prepared to the net and "mu" is decreased by mu_dec.

When one of these situations occurs, the training procedure is stopping:

- The network reaches the max no of epochs (iterations).
- The network exceeds the max number of time.
- The network goal is reached by minimizing the performance.
- The performance of the net gradient decreases under "min_grad".
- mu_max is exceeded by mu value.
- The performance of validation of the net has improved above the "max_fail" times.

**v. The performance** this network use MSE for a network rendering function. It gauge performance of the net according to the mean square error (MSE).

## vi. Testing Stage
When the network successfully trained, then the network become capable of discriminating each of MRI brain tumor image from the others five classes type of brain tumor. The network being available for theclassification process.

## vii. Evaluation stage
To evaluate the performance of the proposed PNN network we use ROC and confusion matrix methods as follow:

**a. ROC evaluation method[4]:**
Compute the "ROC": the curve of Operating Characteristic Receiver to evaluate the performance curvature for the classifier output.
The efficient of proposed algorithm can be calculated by predictive values, There are four predictive values: T positive (TP), T negative (TN), F negative (FN) and F positive (FP). The performance of suggested algorithm results use this formula to calculate which applied in MRI images by specificity, sensitvity, and accuracy of the system

**The sensitivity:** This is the probability of positive result giventhat
Sensitivity = (TP/TP*FP) *10
**The specificity**: This is the probability of negative result
Specificity= (TN/ FN*TN) *10
**Accuracy:** Accuracy is in what way nearby a gauged computed value is for the actual (accurate).
Accuracy =No. of correct data /No. of all data

b. **Confusion matrix**, also named as a matrix of error, is a particular table design that permits to imagining the rendering of an algorithm, usually that are learned in a supervised manner.

## IV. RESULT AND DISCUSSION

First, the noise is removed from the brain tumor MRI images and enhanced with preserved the edges

information. The algorithm depending on morphology filtering (erosion and dilation processes), the structure element shape is disk with radius 15, and the results in figure 2.
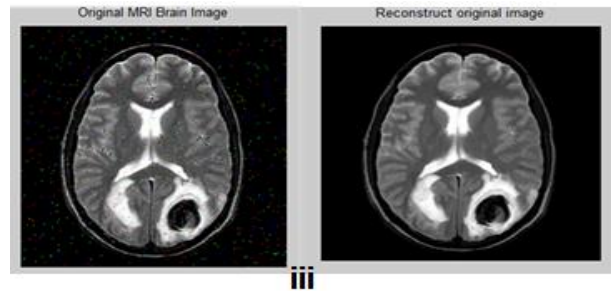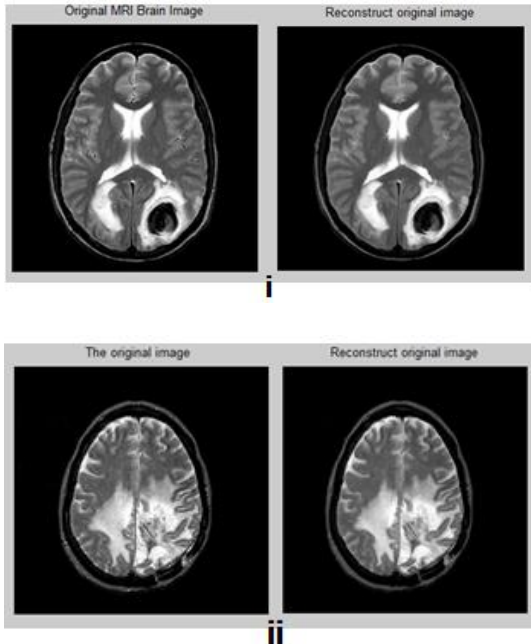






Figure 2: implementing of de-noising algorithm

In the figure (2) i. and ii. the left side image represents the original images and the right side images are the results of applying the algorithm. In iii. of the above figure, the left side represents the original image with noise added for testing, and the right image represents the effect of applying the proposed algorithm.

Table (1) represents the MSE and PSNR values of the above figure (i, ii and iii).

Table1. Values of MSE and PSNR

| Figures | MSE | PSNR |
|---|---|---|
| i. | 25.254089 | 34.107486 |
| ii. | 27.34118 | 34.61122 |
| iii. | 264.9278 | 23.89952 |

The following figures 3 and 4, show the extracted features to four classes of brain tumor MRI images:

| Feature /Class | Saracoma1 | Saracoma2 | Saracoma3 | Saracoma4 | Saracoma5 | Meningioma1 | Meningioma2 | Meningioma3 | Meningioma4 | Meningioma5 |
|---|---|---|---|---|---|---|---|---|---|---|
| mean | 45.30010986 | 46.96894836 | 47.71769714 | 48.32324219 | 44.71122742 | 63.87309265 | 65.04264832 | 64.03793335 | 61.74438477 | 57.39962769 |
| std | 59.10334967 | 61.6054695 | 64.70388326 | 66.94346464 | 62.05939559 | 69.69755713 | 74.033361313 | 75.80909189 | 75.29823777 | 73.09660895 |
| skewness | 1.127666081 | 1.163199983 | 1.279322856 | 1.332745204 | 1.295770846 | 0.536357845 | 0.658913016 | 0.736888771 | 0.763481551 | 0.829538049 |
| kurtosis | 3.542704747 | 3.674610872 | 3.971053989 | 4.023326415 | 3.950331387 | 1.940652248 | 2.147322961 | 2.242209155 | 2.201444173 | 2.25153207 |
| SSQ | 128111982.6 | 137946054.3 | 142476421.8 | 146193858.3 | 124728629.1 | 258053522.9 | 267743361.2 | 259408426.4 | 240875384.7 | 207650327.2 |
| entropy | 0.999967188 | 0.999962899 | 0.999756521 | 0.999201679 | 0.997679567 | 0.989636093 | 0.993864146 | 0.998082672 | 0.999953884 | 0.998358173 |
| IDM | 61708.88 | 61818.64 | 61695.16 | 61814.72 | 61922.52 | 62494.84 | 62526.2 | 62679.08 | 63035.8 | 63374.88 |
| contrast | 2.735232843 | 2.651164216 | 2.745741422 | 2.654166667 | 2.571599265 | 2.133241422 | 2.109221814 | 1.992126225 | 1.718903186 | 1.459191176 |
| Correlation | 0.888356937 | 0.89177583 | 0.887905282 | 0.89157248 | 0.894741065 | 0.911566725 | 0.913100993 | 0.918435966 | 0.929830668 | 0.940325834 |
| Energy | 0.447298974 | 0.448883843 | 0.447209888 | 0.449201691 | 0.451677332 | 0.466061639 | 0.463458481 | 0.462546701 | 0.466222309 | 0.472073839 |
| homogeneity | 0.951156556 | 0.952657782 | 0.950968903 | 0.952604167 | 0.954078585 | 0.961906403 | 0.962335325 | 0.964426317 | 0.9693053 | 0.973943015 |
| SRE1 | 7.414244147 | 7.720602667 | 8.029926555 | 8.346967492 | 8.683997087 | 11.20638154 | 11.47362633 | 11.75733772 | 12.03356922 | 12.33206625 |
| LRE1 | 1367.46696 | 1419.072394 | 1471.114036 | 1524.668622 | 1582.814542 | 2013.575533 | 2055.794068 | 2100.940741 | 2144.474693 | 2192.178771 |
| GLN1 | 18598012.53 | 21122742.16 | 23879401.07 | 26893407.67 | 30214792.85 | 66041930.87 | 71642772.49 | 776680610.61 | 84025750.71 | 90892124.97 |
| RP1 | 64.040802 | 69.85273743 | 75.92674255 | 82.25767517 | 88.8290863 | 150.4398956 | 159.3659363 | 168.5832214 | 178.1013489 | 187.9052734 |
| RLN1 | 7.414244147 | 7.720602667 | 8.029926555 | 8.346967492 | 8.683997087 | 11.20638154 | 11.47362633 | 11.75733772 | 12.03356922 | 12.33206625 |
| LGRE1 | 7.414244147 | 7.720602667 | 8.029926555 | 8.346967492 | 8.683997087 | 11.20638154 | 11.47362633 | 11.75733772 | 12.03356922 | 12.33206625 |
| HGRE1 | 696.5103381 | 725.1070281 | 754.0530452 | 783.8884402 | 815.6135774 | 1052.678106 | 1078.607364 | 1106.569906 | 1134.246696 | 1164.342935 |

Figure 3: Features values extracted from samples of Sarcoma & Meningioma brain tumor MRI.

**DOI 10.17148/IJARCCE.2017.6125**

| Feature /Class | Asrtrocytoma1 | Asrtrocytoma2 | Asrtrocytoma3 | Asrtrocytoma4 | Asrtrocytoma5 | Benign1 | Benign2 | Benign3 | Benign4 | Benign5 |
|---|---|---|---|---|---|---|---|---|---|---|
| mean | 38.98132324 | 40.15216064 | 40.96209717 | 41.17784119 | 42.75073242 | 75.7861366 | 57.75235438 | 67.1478321 | 114.4692326 | 75.13841242 |
| std | 59.98200426 | 62.44609714 | 64.03494671 | 65.5939562 | 68.47390212 | 69.47591934 | 46.7835287 | 52.69070543 | 55.36270754 | 66.82020913 |
| skewness | 1.426746904 | 1.451297371 | 1.44908691 | 1.490330202 | 1.468762467 | 0.507399799 | 0.721353559 | 0.632438404 | 0.62276372 | 0.798545738 |
| kurtosis | 4.106536224 | 4.184857054 | 4.095570501 | 4.184551969 | 3.982762778 | 2.198718816 | 3.840735396 | 3.293519227 | 2.882180323 | 2.887920114 |
| SSQ | 94171682.15 | 100067169.1 | 104250150 | 105378822.5 | 113791112.4 | 218248728.1 | 162039943.6 | 220526998.8 | 647162407.7 | 275869545.6 |
| entropy | 0.9900969 | 0.98305768 | 0.983888752 | 0.97630166 | 0.981573639 | 0.136286949 | 0.563069362 | 0.618095142 | 0.034856283 | 0.024856283 |
| IDM | 60307.48 | 60924.88 | 60952.32 | 61325.7 | 60759.26 | 37965.56 | 48785.12 | 47691.28 | 50264 | 49997.92 |
| contrast | 3.808609069 | 3.335723039 | 3.314705882 | 3.028722426 | 3.462576593 | 1.353646661 | 1.515483999 | 2.687222222 | 0.201354459 | 0.191352859 |
| Correlation | 0.842498791 | 0.860716815 | 0.861752292 | 0.872345818 | 0.855117437 | 0.263400407 | 0.863282929 | 0.786240697 | 0.672236 | 0.207720003 |
| Energy | 0.434816427 | 0.447799192 | 0.447611997 | 0.457806017 | 0.446590896 | 0.935633844 | 0.743807727 | 0.69161341 | 0.601613411 | 0.991181074 |
| homogeneity | 0.931989124 | 0.940433517 | 0.940808824 | 0.945915671 | 0.938168275 | 0.975827738 | 0.972937786 | 0.952013889 | 0.899582983 | 0.996582985 |
| SRE1 | 14.04706692 | 14.40475137 | 14.75375905 | 15.12097419 | 15.48733587 | 2.591446715 | 2.973569411 | 3.221525671 | 3.560082588 | 3.852896484 |
| LRE1 | 2474.23784 | 2533.463268 | 2591.369625 | 2652.928651 | 2714.802243 | 176.3175175 | 208.4071154 | 218.0788592 | 243.826211 | 257.6221326 |
| GLN1 | 133108951 | 143002141.7 | 153282958.7 | 164220059.5 | 175660016.6 | 731689.2859 | 1078085.22 | 1471054.227 | 1998147.155 | 2615133.892 |
| RP1 | 240.8343048 | 252.1409607 | 263.6942596 | 275.4790192 | 287.4950714 | 11.80423038 | 11.77142688 | 14.77819259 | 18.18638632 | 21.99008507 |
| RLN1 | 14.04706692 | 14.40475137 | 14.75375905 | 15.12097419 | 15.48733587 | 2.591446715 | 2.973569411 | 3.221525671 | 3.560082588 | 3.852896484 |
| LGRE1 | 14.04706692 | 14.40475137 | 14.75375905 | 15.12097419 | 15.48733587 | 2.591446715 | 2.973569411 | 3.221525671 | 3.560082588 | 3.852896484 |
| HGRE1 | 1338.590483 | 1374.80689 | 1410.194224 | 1447.410231 | 1484.679052 | 236.7662016 | 271.0035896 | 291.1502445 | 323.4975411 | 351.7512079 |

Figure 4: Features values extracted from samples of Astrocytoma & benign brain tumors MRI.

Figure (5) shows the architecture of the configured network. The network consists of 13 input neurons (number of features that used in the classification process), two hidden layers the first have 10 neurons and the seconds have 5 neurons, and last the output layer of five nodes (these five nodes represent the number of classes that the network will classify the output to them).
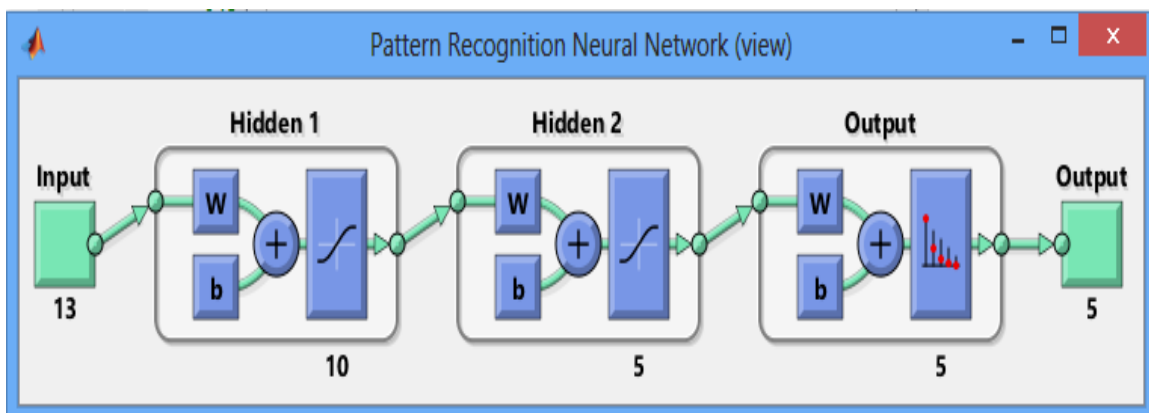


Figure (5) : PNN Architecture.

In the training phase, the network trained on samples (input,target). Inputs represent 13 selected features that extracted from each of five classes of brain tumor MRI images that the network tries to classify to them. Each vector of the target has only one 1 in the neuron that the sample belongs to it. Figure 7 explains how the PNN trained depending on setting parameters, the net trained at 32 epoch to reach minimum gradient.
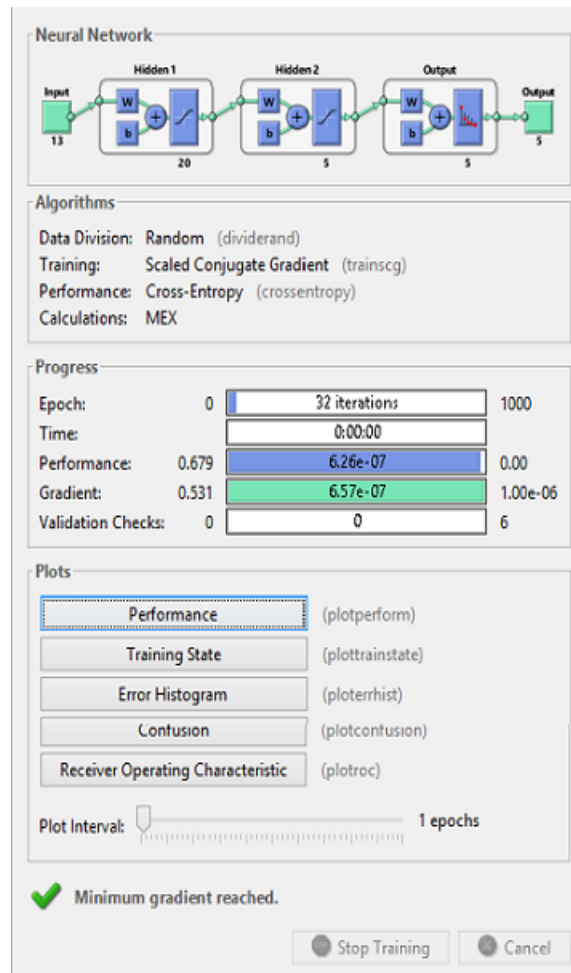
Figure 6: PNN Architecture& Training Parameters

**PNN classification evaluation**

The evalution of the perofmance and accuracy of the proposed PNN is dpending on the following:

1. The first method is to test the network on the same sample features that trained on, then show the network how to classify them. Figure 7 shows that the network classifies each sample feature exactly to there class type.

| Column | Column2 | Column3 | Column4 | Column5 | Column6 | Column7 | Column8 | Columr | Column | Column1 | Column1 |
|---|---|---|---|---|---|---|---|---|---|---|---|
| 0.999999 | 0.99999888 | 0.99999882 | 0.99999879 | 0.9999989 | 0.9999988 | 5.55E-07 | 5.68E-07 | 5.68E-07 | 5.56E-07 | 5.58E-07 | 5.27E-07 |
| 7.23E-07 | 6.90E-07 | 5.24E-07 | 5.22E-07 | 5.99E-07 | 8.40E-07 | 0.99999889 | 0.9999989 | 0.999999 | 0.999999 | 0.9999989 | 0.9999989 |
| 1.20E-09 | 1.29E-09 | 2.40E-09 | 2.61E-09 | 1.83E-09 | 1.12E-09 | 4.00E-07 | 4.00E-07 | 4.00E-07 | 3.98E-07 | 3.97E-07 | 4.17E-07 |
| 2.56E-07 | 2.68E-07 | 3.90E-07 | 4.00E-07 | 3.27E-07 | 2.31E-07 | 6.22E-14 | 6.25E-14 | 6.24E-14 | 6.15E-14 | 6.19E-14 | 6.26E-14 |
| 1.56E-07 | 1.63E-07 | 2.68E-07 | 2.83E-07 | 2.06E-07 | 1.34E-07 | 1.59E-07 | 1.64E-07 | 1.65E-07 | 1.62E-07 | 1.63E-07 | 1.53E-07 |

| Column | Column14 | Column1 | Column16 | Column1 | Column1 | Column1 | Column. | Column. | Column22 | Column2 | Columr |
|---|---|---|---|---|---|---|---|---|---|---|---|
| 5.48E-07 | 5.63E-07 | 5.48E-07 | 5.53E-08 | 4.63E-08 | 3.86E-08 | 3.14E-08 | 3.57E-08 | 3.67E-08 | 2.42E-08 | 2.34E-08 | 2.72E-08 |
| 0.999999 | 0.99999879 | 0.9999989 | 4.97E-07 | 6.04E-07 | 6.77E-07 | 8.50E-07 | 6.71E-07 | 7.10E-07 | 1.14E-06 | 1.12E-06 | 8.52E-07 |
| 4.12E-07 | 4.68E-07 | 4.05E-07 | 0.999998957 | 0.9999989 | 0.9999989 | 0.9999987 | 0.9999989 | 0.9999988 | 0.999998534 | 0.9999986 | 0.999999 |
| 6.30E-14 | 6.83E-14 | 6.34E-14 | 4.82E-07 | 4.39E-07 | 4.15E-07 | 3.65E-07 | 4.17E-07 | 4.29E-07 | 2.81E-07 | 2.87E-07 | 3.25E-07 |
| 1.64E-07 | 1.82E-07 | 1.60E-07 | 8.84E-09 | 1.03E-08 | 1.09E-08 | 1.33E-08 | 1.03E-08 | 1.02E-08 | 1.89E-08 | 1.82E-08 | 1.41E-08 |

| Column25 | Column2 | Column | Column28 | Column29 | Column30 | Column31 | Column32 | Column33 | Column34 | Column35 | Column36 |
|---|---|---|---|---|---|---|---|---|---|---|---|
| 2.95E-08 | 6.88E-07 | 5.82E-07 | 6.42E-07 | 5.82E-07 | 5.65E-07 | 6.28E-08 | 1.22E-06 | 0.000508158 | 7.30E-08 | 6.98E-08 | 6.92E-08 |
| 7.30E-07 | 8.83E-13 | 5.55E-13 | 8.61E-13 | 5.55E-13 | 5.30E-13 | 9.70E-08 | 3.56E-07 | 6.23E-07 | 1.06E-07 | 1.02E-07 | 1.03E-07 |
| 0.999998875 | 7.69E-07 | 9.34E-07 | 8.29E-07 | 9.34E-07 | 9.64E-07 | 5.12E-09 | 2.85E-08 | 7.34E-07 | 5.87E-09 | 5.78E-09 | 5.51E-09 |
| 3.53E-07 | 0.999998 | 0.999998 | 0.999997944 | 0.999997901 | 0.999997868 | 7.19E-07 | 2.13E-06 | 0.000211665 | 6.72E-07 | 6.59E-07 | 7.06E-07 |
| 1.21E-08 | 5.31E-07 | 5.83E-07 | 5.86E-07 | 5.83E-07 | 6.04E-07 | 0.999999116 | 0.99999627 | 0.999278821 | 0.999999143 | 0.99999916 | 0.999999117 |

Figure 7: performance array after testing PNN on same training features

2. Using the validation vectors to end the training phase as soon as the performance of the network on these vectors of validation is unsuccessful to advance the network behaviour or stay unchanged for a number of fails epochs. Then using the test vectors to examine that the network is generalizing in a good manner, on the other hand, do not have any influence on training. The figure 4.8 below shows how the gradient is decreasing until it reaches the minimum at epoch 10, also it shows Mu value decreasing and in the end show the valdiation chechs.
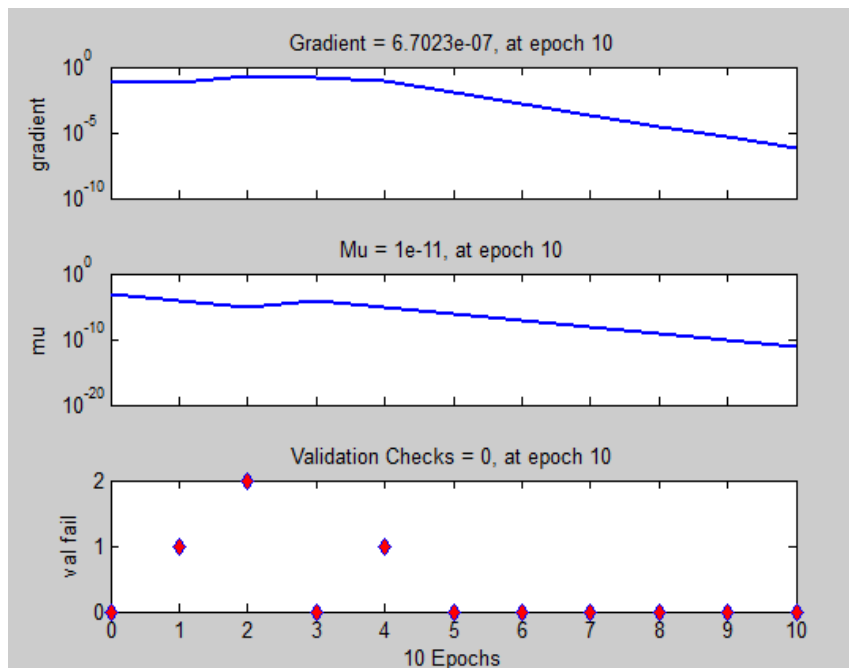


Figure 8: Training State of the network at 10 epochs
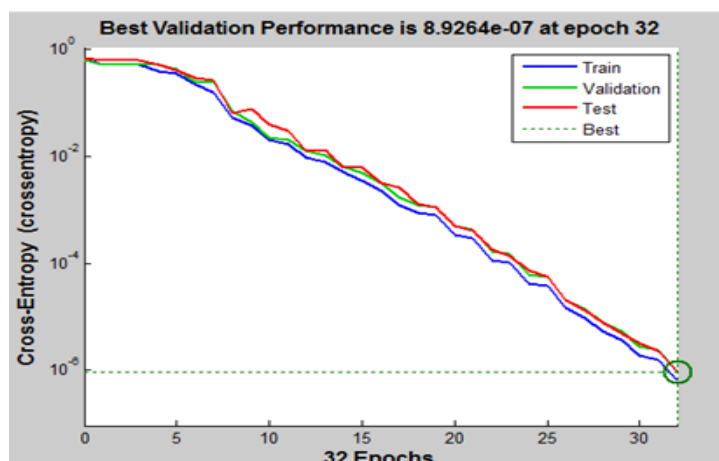


Figure 9: Network performance.

Figure 9 shows the network behaviour in the training, validation, and test stages. Also, figure 10 describes error histogram of th network throgh the training phase.
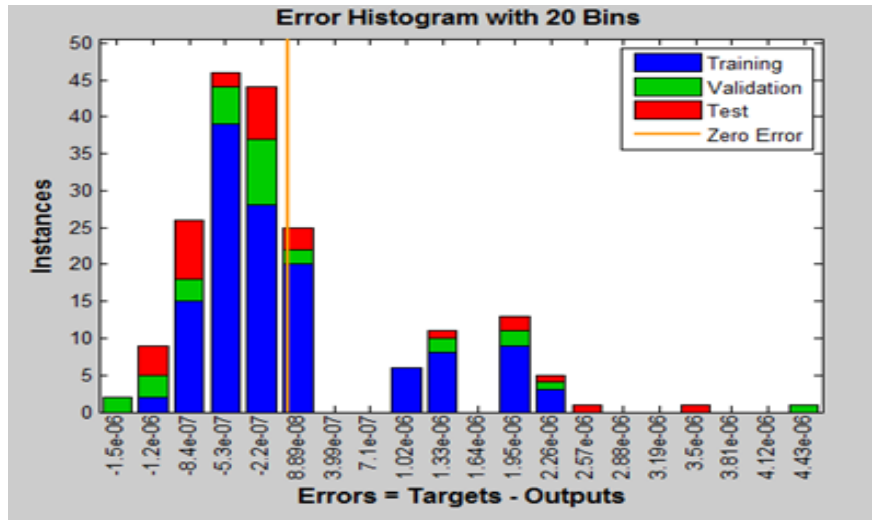


Figure 10: Error histogram.

1. Confusion matrix. It shows the different kinds of errors that happened for the last trained network. The number of states that were classified in a correct way is showed in diagonal cells, and the misclassified states are showed at the off-diagonal cells. The whole percentage of correctly classified states (cell with green color) is showed in a cell with a blue color in the bottom right and finally, the total percentage of states that misclassified are in a cell with red color.

The next figures (11 and 12) displays the matrixes of confusion to train, test, and validate, and then how the four kinds of data are joined. These figures illustrate how the networks outputs have a very good precise, such as you can see by the high no. of accurate replies in the cells with green and the low no. of inaccurate replies in the cells with red. Overall accuracies are clarified in a bottom right blue cell.
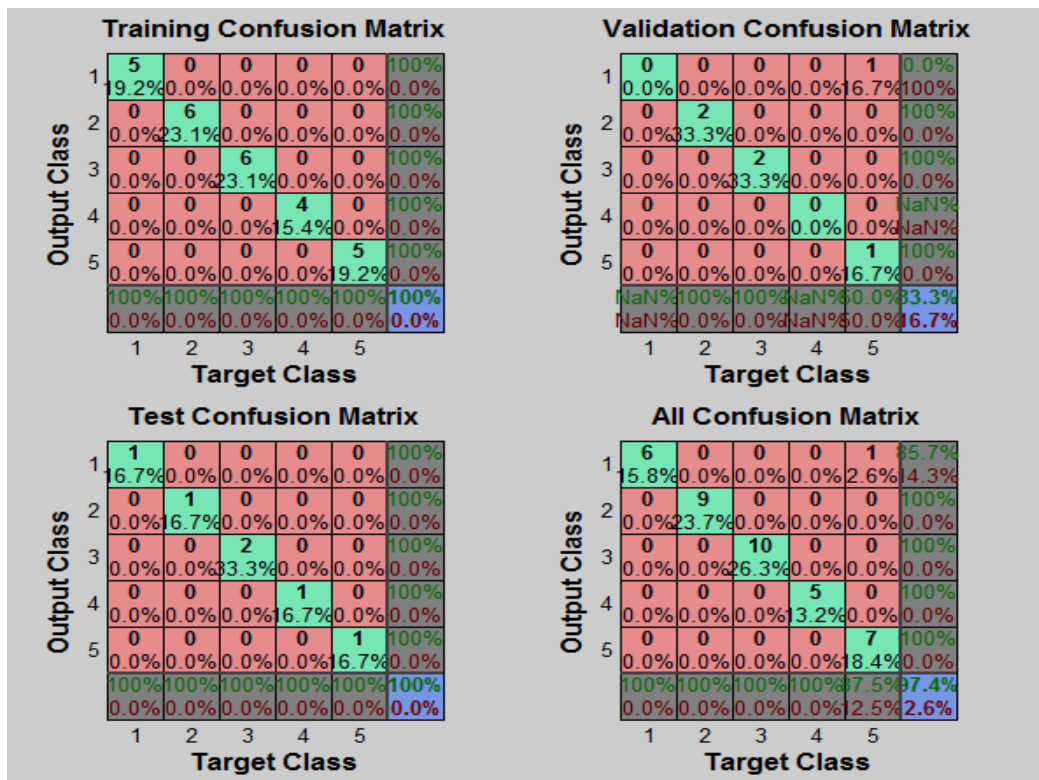


Figure 11: Confusion matrix of best feature.
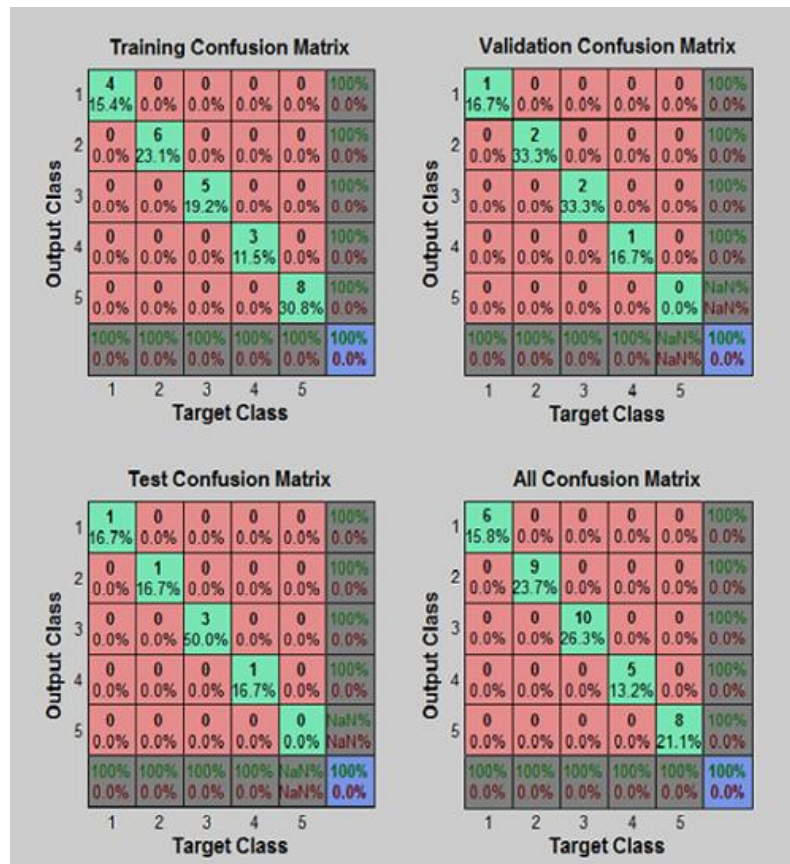
Figure 12: Confusion matrix of Network Test.

Generally the classification accuracy using the proposed method is comparable or higher than in other.The evaluation of the proposedmethod gives good accuracy in diagnosis between five classes of tumour (98% in average of all diagnosis).

In [9], LSFT enhanced the performance of the PNN, achieving classification accuracies of 95.24% for discriminating between metastatic and primary tumors and 93.48% for distinguishing gliomas from meningiomas (94 % accuracy in average). In [10] the method was applied on a population of 102 brain tumors histologically diagnosed as metastasis (24), meningiomas (4), gliomas WHO grade 2 (22), gliomas WHO grade 3 (18), and glioblastomas (34). The binary SVM classification accuracy, sensitivity, and specificity, assessed by leave-one-out cross-validation, were respectively 85%, 87%, and 79% for discrimination of metastases from gliomas, and 88%, 85%, and 96% for discrimination of high grade (grade III and IV) from low grade (grade II) neoplasms (87 % accuracy in average).

## V. CONCLUSION

This paper proposed new method for brain tumour classification, at first stage MR image enhanced and improved based on mathematical morphology. Simulation results show significant improvement in contrast of MR images depending on results from quality metric (mse and psnr).The pattern neural network PNN classifier is implemented and used to classify the MRI brain tumour images into benign, Sarcoma, Meningioma, Glioma and Anaplastic Astrocytoma,the PNN net trained on the features that are selected from extracted features, then the net is tested and evaluated. Later the net used for classification of MRI brain tumour images into these type of brain tumour.

Future work should focus on the following directions: The implemented algorithms can be employed for MR images with another contrast mechanisms such as proton-density-weighted, and diffusion weighted images. Improve the classification accuracy by extracting more efficient features and increasing the training data set.

## REFERENCES

[1]  Mustaqeem, et al., "An Efficient Brain Tumor Detection Algorithm Using Watershed &Thresholding Based Segmentation" International Journal of Image, Graphics and Signal Processing, Vol.4, No.10, 2012, pp34-39.

[2]  M. Madheswaran and D. Anto, "Classification of brain MRI images using support vector machine with various Kernels" Biomedical Research, Madheswaran/Dhas 2015 Volume 26 Issue 3

[3]  P.Muthu Krishnammal , "Automated Brain Image classification using Neural Network Approach and Abnormality Analysis "International Journal of Engineering and Technology (IJET) Vol 7 No 3 Jun-Jul 2015.

[4]  Said Charfi, Redouan & Lahmyed & Lalitha. "A novel approach for brain tumor detection using neural network". International Journal of Research in Engineering & Technology (IMPACT: IJRET) ISSN(E): 2321-8843; ISSN(P): 2347-4599 Vol. 2, Issue 7, Jul 2014, 93-104 © Impact Journals.

[5]   Ed-Edily Mohd. Azhari, Muhd. Mudzakkir Mohd. Hatta, Zaw Zaw Htike, and Shoon Lei Win, aninternational journal of information technology convergence and services (IJITCS), vol. 4., no. 1, 2014.

[6]   A.LAKSHMI, Dr.T.ARIVOLI "Computer Aided Diagnosis system for brain tumor detection and segmentation", Journal of Theoretical and Applied Information Technology 20th June 2014. Vol. 64 No.2 © 2005 - 2014 JATIT & LLS.

[7]   Nalbalwar, R., U. Majhi, R. Patil and S. Gonge, 2014. Detection of brain tumor by using ANN. Int. J. Res. Advent Technol., 2(4): 279-282.

[8]   John, P., Brain tumor classification using wavelet and texture based neural network.2012, Int. J. Sci. Eng. Res., 3(10): 1-7.

[9]   Georgiadis P, Cavouras D, Kalatzis I, Daskalakis A, Kagadis GC, Sifaki K, Malamas M, Nikiforidis G, Solomou E. Improving brain tumor characterization on MRI by probabilistic neural networks and non-linear transformation of textural features. Computer Methods and Programs in Biomedicine. 2008;89:24–32.

[10]  Evangelia I. Zacharaki "Classification of brain tumor type and grade using MRI texture and shape in a machine learning scheme" Magn Reson Med. 2009 Dec; 62(6): 1609–1618.

[11]  P. Mohanaiah, P. Sathyanarayana, L. GuruKumar " Image Texture Feature Extraction Using GLCM Approach" International Journal of Scientific and Research Publications, Volume 3, Issue 5, May 2013 1 ISSN 2250-3153

[12]  P. Garg, "Evolutionary Computation Algorithms for Cryptanalysis: A Study", India, (IJCSIS) ,Vol. 7, No. 1, 2010.

[13]  D. Brodi´c, Z.N. Milivojevi´c, and C.A. Maluckov. Recognition of the script in serbian documents using frequency occurrence and co-occurrence analysis. The Scientific World Journal, 2013, no. 896328:1–14, 2013.

[14]  D. Brodi´c, Z.N. Milivojevi´c, and Alessia Amelio, "Analysis of the South Slavic Scripts by Run-Length Features of the Image Texture" arXiv:1507.04908 v1 [cs.CV] 17 Jul 2015.

[15]  Victo Sudha George and V. Cyril Raj "Accurate and Stable Feature Selection Powered by Iterative Backward Selection and Cumulative Ranking Score of Features" Indian Journal of Science and Technology, Vol 8(11), DOI: 10.17485/ijst/2015/v8i11/71766, June 2015

[16]  Namita Aggarwal, R. K. Agrawal "First and Second Order Statistics Features for Classification of Magnetic Resonance Brain Images" Journal of Signal and Information Processing, 2012, 3, 146-153

[17]  Karpagam Tirumazhisai Manivannan "Development of Gray Level Co-occurrence Matrix based Support Vector" The University of Toledo August 2012.

[18]  Mohammad Alam Mia, Shovasis Biswas, Monalisa Urmi, Abubakar Siddique "An Algorithm For Training Multilayer Perceptron (MLP) For Image Reconstruction Using Neural Network Without Over fitting" International Journal of Scientfic & Technology Reserch volume 4, issue 02, FEBRUARY 2015.